# Polyelectrolyte−Multicomponent Lipid Bilayer Interactions. Unusual Effects on Going from the Dilute to the Semidilute Regime

**Antonio Raudino* and Francesco Castelli**

*Dipartimento di Scienze Chimiche, Universitá di Catania, Viale A. Doria 6-95125, Catania, Italy*

*Received June 21, 1996; Revised Manuscript Received January 3, 1997*[⊗]

ABSTRACT: We present a theoretical model of two-component lipid membranes in close contact with a polyelectrolyte solution. Fluid mixtures of charged and neutral lipids as well as oppositely charged polyelectrolytes were considered, the lipids being allowed to redistribute themselves in order to maximize their interaction with the polymer. In the dilute regime the adsorption of a polyelectrolyte onto oppositely charged lipid surfaces induces lateral phase separation of the charged lipids, which form clusters near the polymer adsorption sites. On raising the polymer concentration to the semidilute regime (overlapping chains) the polyelectrolyte solution forms a homogeneous ionic background interacting with the membrane lipid heads. Naively one might guess that a redissolution of the clusters would then take place because of electrostatic repulsion and entropic effects. A mean-field model of the short-range polymer−surface interactions, augmented with the possibility of polymer lateral density variations, is proposed. We assume that only one kind of lipid can favorably bind to the polyelectrolyte, while the other ones do not exhibit any interaction with the polyelectrolyte. For ideal chains the model predicts the onset of slowly decaying attraction forces among nearby lipidic clusters which are simultaneously interacting with polymer chains (force ∝ (distance)$^{-2}$). The force between lipid clusters is entropic in nature and is due to the deformation of the polymer density at the membrane−water interface. Inclusion of excluded volume effects greatly reduces the magnitude of the attractive forces which now decay exponentially. The model also suggests very slow kinetics for the clustering process, characterized by a long latency period followed by a burst in the aggregation rate when the process is near completion. Preliminary differential scanning calorimetry (DSC) measurements performed on lipid vesicles suspended in aqueous solutions of polyelectrolyte support the theoretical predictions, showing the onset of a permanent lateral phase separation in dilute polymer solutions which remains stable on further raising the polymer concentration to the semidilute or even concentrated regime.

## 1. Introduction

Polyelectrolyte-induced formation of microdomains in multicomponent membranes, leading to patches richer in charged lipids, is a phenomenon which has been known for a long time. Experimental approaches like electron spin resonance spectroscopy,[1] NMR,[2] scanning calorimetry[3−6] and dilatometry,[7] and freeze-fracture electron microscopy[8] have been widely used to detect them in model membranes and living cell surfaces, but only a few attempts to model the effect have been reported in the literature. Recently, we reported calorimetric measurements together with simple model calculations in the limit of very dilute polyelectrolyte solutions where the chains can be considered as independent units.[5,6]

In the dilute regime microdomain formation is easily understood in terms of charged lipid enrichment near the polyelectrolyte binding region, provided lipid mobility is nonvanishing and polymer and ionic lipids bear opposite charges. Here, the energy loss due to clustering of identically charged lipids is largely compensated for by the increased number of polymer−lipid contact sites. Then, clustering of lipids, spanning of single polyelectrolyte chains,[5,9] and an overall increase in the number of adsorbed chains[5] are all likely events in multicomponent fluid membrane−polymer systems (Figure 1, case A).

More intriguing is the behavior of a multicomponent membrane in the semidilute regime. Indeed, on further raising the polymer concentration to the chain overlap region, the charged lipids "see" a homogeneous background of ionic sites available for binding. There is no longer a net energy gain in forming aggregates of charged objects; hence the clusters become unstable and should redissolve, forming a homogeneous melt of charged and neutral lipids. This is case B in Figure 1.

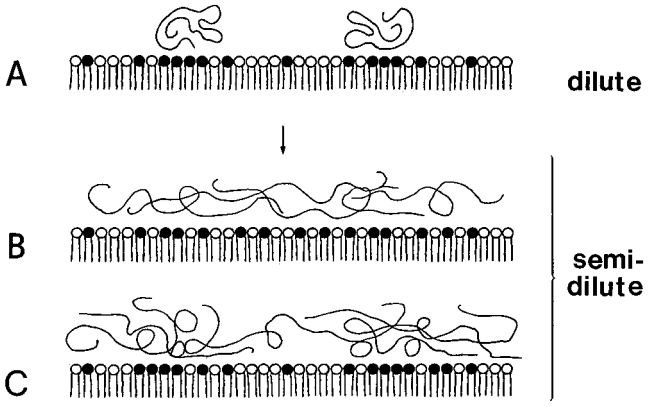


**Figure 1.** Schematic representation of a polymer−multicomponent membrane system in the dilute (upper drawing) and semidilute (lower drawing) regime. Black and white circles describe neutral and charged lipid heads, respectively. Polymer and lipids bear opposite charges.

Let us investigate what happens when one introduces charged lipid−polymer interactions, while also assuming that no interactions at all exist among polymer and neutral lipids. Polymer binding to a single lipid, or to a small cluster of lipids, perturbs the local polymer density at the interface, so that two nearby lipid clusters

* Corresponding author.
[⊗] Abstract published in *Advance ACS Abstracts,* March 1, 1997.

S0024-9297(96)00904-7 CCC: $14.00 

feel a different environment depending upon their mutual distance. In order to minimize the free energy, the system may find it more convenient to modify the distance between the clusters (provided the clusters are free moving within the lipid matrix) instead of, for instance, reducing the deformation of the polymer profile at the interface. Therefore, even in the absence of any direct cluster−cluster interaction, there may exist an indirect force among the cluster particles (Figure 1, case C), which gives rise either to a redissolution (repulsive force) or to a further extensive aggregation (attractive force) depending on the details of the particle−polymer solution interactions.

In the past, several authors have treated the problem of solvent-mediated interactions among noninteracting particles (in vacuo) embedded in a homogeneous structured fluid. It has been demonstrated that long-range interactions, usually termed structural forces, naturally emerge as a consequence of a distance-dependent perturbation of the order parameter in the case of two rigid bodies within a fluid. After the pioneering work of Marcelja and Radic,[10] these ideas have been successfully applied to many biophysical problems such as, for instance, understanding the origin of attractive forces among lipid-soluble proteins[11] as well as the repulsive interactions between neutral lipid membranes brought at close distance.[12]

To our knowledge, the present model addresses for the first time a related but new kind of indirect force among membrane components, and preliminary calorimetric measurements performed in our laboratory seem to support the validity of the model.

These forces could be widespread in biological systems because membrane cells contain several different kinds of lipids interacting in the cell interior with a rather concentrated solution of charged water-soluble proteins (cytosol), but no attempt to present experimental evidence of this phenomenon in biological systems will be made in this paper.

## 2. Materials and Methods

Membrane-forming lipids were selected among the most common and investigated phospholipids. The neutral L-α-dipalmitoylphosphatidylcholine (DPPC)[13] was obtained from Fluka (puriss), while the negatively charged L-α-dipalmitoylphosphatidic acid[13] (DPPA) was obtained from Sigma and checked for purity by bidimensional thin-layer chromatography. The phospholipid's phosphorus content was assayed as inorganic phosphate by an analytical procedure previously reported.[14]

Poly(L-lysine) (MW = 20 000) was purchased from Sigma and used without further purification.

Large multilamellar vesicles were prepared as follows. Lipid solutions in $CH_3Cl/CH_3OH$ (1:1 v/v) were mixed to obtain homogeneous mixtures at different molar ratios. The solvents were removed in a stream of nitrogen in a rotoevaporator at 35 °C, and the resulting film was lyophilized for 3 h. The lipid mixtures (ca. 14 μmol of total lipids) were added to 250 μL of buffered 50 mM Tris (pH 7). A concentrated stock solution of poly(L-lysine) was then added to the lipid suspension. The ionic strength, adjusted by NaCl, was held constant at $10^{-1}$ M, and some experiments were performed at higher ionic strengths. The samples were vortexed twice and shaken for 3 h at 70 °C in a water bath in order to form large multilamellar lipid vesicles. Afterward aliquots of 120 μL were transferred and sealed in aluminum pans. After the DSC runs, the phosphorus content of the lipid samples was determined as above.

Differential scanning calorimetry (DSC) was performed with a Mettler TA 3000 calorimeter, equipped with a DSC 30 cell and a TC 10 processor. The sensitivity was 17.1 mW full scale, using Tris buffer as reference. The samples were analyzed by using heating and cooling rates of 2 °C/min in the temperature range 10−80 °C. Each sample was heated and cooled through the lipid phase transition region at least four times to ensure constant thermotropic behavior. Palmitic acid was employed to calibrate the temperature scale and the transition enthalpies ($\Delta H$). Enthalpies were evaluated from the peak areas using the integration program of the TA processor. The areas calculated lie within the experimental error (±5%).

## 3. Theory

**3.1. Interfacial Free Energy Functional.** In the Cahn−de Gennes picture[15] the surface energy associated with the adsorption of a polymer from a semidilute solution can be written as

$$U = U^{(\circ)} - \gamma \int_S \Phi \, dS + \int_V (F(\Phi) + C(\Phi)(\nabla\Phi)^2) \, dV \quad (1)$$

where the first integral represents the contact energy between the polymer solution and the surface and the second integral represents the contribution from distortion of the concentration profile. $U^{(\circ)}$ is the surface energy of pure solvent, $\Phi$ is the local polymer volume fraction (tending to a constant value $\bar{\Phi}$ far from the interface), $\gamma$ is the sticking energy of the polymer per unit area ($\gamma > 0$ for adsorption), $F(\Phi)$ is the homogeneous part of the free energy density, and $C(\Phi)$ describes the "stiffness" of the polymer solution to spatial deformation of the concentration. In semidilute polymer solution ($\Phi \ll 1$ but still large enough to allow for polymer chain overlapping) an analytical expression for $C(\Phi)$ is

$$C(\Phi) = \frac{k_B T}{a^3} b \frac{a^2}{\Phi} \quad (2a)$$

where $k_B$ is the Boltzmann constant, $T$ is the absolute temperature, $a$ is the monomer size, and $b$ is a model-dependent numerical constant (equal to $^1/_{36}$ in the weak segregation limit,[15,16] $^1/_{24}$ in the strong segregation limit,[17,18] and $^5/_{48}$ for the cubic lattice model;[19] the value $^1/_{24}$ will be used throughout this paper). In the mean-field approximation, $F(\Phi)$ takes the usual virial expansion form:[15]

$$F(\Phi) = \frac{k_B T}{a^3}\left(\frac{\Phi}{N}\log\Phi + \frac{1}{2}\varphi\Phi^2 + O(\Phi^3)\right)$$

$$\cong \frac{k_B T}{a^3}\frac{1}{2}\varphi\Phi^2 \quad (2b)$$

where $\varphi$ is a dimensionless excluded volume parameter ($\varphi > 0$ in good solvents) and $\Phi$ is the polymer volume fraction. The last approximation in eq 2b follows in semidilute solution for large $N$; otherwise the logarithmic term must be retained. As usual, the functional can be simplified by using the order parameter $\psi^2 = \Phi$. The equations governing the concentration profile are determined by minimizing eq 1 subject to the constraints $\int_V \psi^2 \, dV =$ constant and $\psi \cong \bar{\Phi}^{1/2}$ as $r$ goes to infinity, resulting in the standard Euler−Lagrange equation in the new variable $\psi$:

$$\frac{a^2}{6}\nabla^2\psi - \varphi\psi^3 + \varphi\bar{\psi}^2\psi = 0 \quad (3)$$

where $\bar{\psi}^2 = \bar{\Phi}$ is the bulk concentration. The boundary condition at the interface is slightly different from that

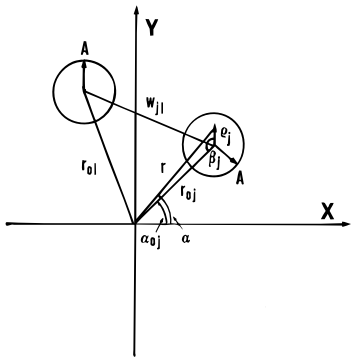


**Figure 2.** Geometrical parameters used to define a cluster distribution over the $X-Y$ plane (the membrane plane). The clusters are described as identical disks of radius $A$, the centers of which are a distance $w_{jl}$ apart.

generally used for polymer adsorption onto a laterally homogeneous surface. A suitable expression, which generalizes the well-known boundary condition introduced by de Gennes,[15] is

$$\frac{1}{\psi}\frac{\partial\psi}{\partial z}\bigg|_{z=0} = -\kappa \qquad r, \alpha \in I_A \tag{4a}$$

$$\frac{1}{\psi}\frac{\partial\psi}{\partial z}\bigg|_{z=0} = 0 \qquad r, \alpha \in I_B \tag{4b}$$

provided the surface−polymer energy of interaction is short-ranged. $\kappa \equiv 6\gamma a/k_BT$ is a measure of the sticking energy, $r$, $z$, and $\alpha$ are the cylindrical coordinates defined in Figure 2(the $z$-axis is perpendicular to the $X-Y$ plane) and the symbols $I_A$ and $I_B$ label two mutually exclusive domains for the variables $r$ and $\alpha$. In particular, $I_A$ contains all the points over the plane $z = 0$ lying inside the disks of radius $A$, whereas $I_B$ is representative of all the remaining points outside the disks.

Particularly simple expressions are obtained in the limit of small sticking energies ($\kappa \cong 0$); in that case we may follow a perturbation procedure. Letting $\psi = \psi^{(0)} + \psi^{(1)} + ... = \bar{\Phi}^{1/2} + \psi^{(1)} + ...$, $\kappa \equiv \kappa^{(1)}$ and making use of eqs 3 and 4, we find after simple rearrangement

$$\nabla^2\psi^{(1)} - \nu^2\psi^{(1)} = 0 \tag{5}$$

$\nu^2 \equiv (12\varphi/a^2)\bar{\Phi}$. In polar coordinates

$$\nabla^2 \equiv \frac{\partial^2}{\partial r^2} + \frac{1}{r}\frac{\partial}{\partial r} + \frac{\partial^2}{\partial z^2} + \frac{1}{r^2}\frac{\partial^2}{\partial \alpha^2}$$

and the boundary conditions become

$$\lim_{r\to\infty} \psi^{(1)} = 0 \tag{6a}$$

$$\frac{\partial\psi^{(1)}}{\partial z}\bigg|_{z=0} = -\kappa^{(1)}\bar{\Phi}^{1/2} \qquad r, \alpha \in I_A \tag{6b}$$

$$\frac{\partial\psi^{(1)}}{\partial z}\bigg|_{z=0} = 0 \qquad r, \alpha \in I_B \tag{6c}$$

The solution of eq 5 together with the boundary conditions (6a−c) yields the polymer profile near a patterned interface of attractive and repulsive domains.

**3.2. Calculation of the Polymer Profile.** A general solution of eq 5 which vanishes at $z \to \infty$ is

$$\psi^{(1)} = A_0^{(1)} + \sum_{n=-\infty}^{+\infty}\int_0^\infty A_n^{(1)}(\lambda)J_n(\lambda r)\exp(-z(\lambda^2 + \nu^2)^{1/2})e^{+in\alpha}\,d\lambda + \text{C.C.} \tag{7}$$

where $J_n(X)$ is a Bessel function of order $n$ and the coefficients $A_n^{(1)}$ are to be determined by applying the boundary conditions. From eq 6a it follows that $A_0^{(1)} = 0$. Combining eqs 6b,c and 7, one finds

$$\sum_{n=-\infty}^{+\infty}\int_0^\infty A_n^{(1)}(\lambda)J_n(\lambda r)(\lambda^2+\nu^2)^{1/2}e^{+in\alpha}\,d\lambda = \begin{cases}\kappa^{(1)}\bar{\Phi}^{1/2} & r, \alpha \in I_A \\ 0 & r, \alpha \in I_B\end{cases} \tag{8}$$

where the domains $I_A$ and $I_B$ have been defined in section 3.1. It is very difficult to solve eq 8 for $A_n^{(1)}$. However, through a proper change of variables which makes use of local coordinates the origin of which is set at the centers of the attractive circular domains (see Figure 2), we derived in Appendix A an exact analytical result. Here we quote the final result:

$$A_n^{(1)}(\lambda) = \kappa^{(1)}\bar{\Phi}^{1/2}\frac{A}{(\lambda^2+\nu^2)^{1/2}}J_1(\lambda A)\sum_{j=1}^{M}\exp(-in\alpha_{0j})\,J_n(\lambda r_{0j}) \tag{9}$$

where the sum in the right hand side of eq 9 spans over the $M$ circular domains of radius $A$, the centers of which ar located at $r_{01}$, $\alpha_{01}$; ...; $r_{0j}$, $\alpha_{0j}$; ...; $r_{0M}$, $\alpha_{0M}$ (see Figure 2).

Once the coefficients $A_n^{(1)}(\lambda)$ have been calculated, they can be used to evaluate the profile $\psi^{(1)} = \psi^{(1)}(r,z,\alpha)$ by means of eq 7.

**3.3. Calculation of the Interfacial Energy.** The knowledge of the polymer profile allows us to calculate by eq 1 the adsorption energy onto a patched surface. In the limit of weak sticking energy $\gamma$, a straightforward calculation gives the first-order energy term:

$$U_{TOT}^{(1)} = U_S^{(1)} + U_V^{(1)} = -2\gamma\bar{\Phi}^{1/2}\int_S\psi^{(1)}\,dS + 2\varphi\frac{k_BT}{a^3}\bar{\Phi}^{3/2}\int_V\psi^{(1)}\,dV + O(\psi^{(1)^2}) \tag{10}$$

where in deriving eq 10, we exploited the condition $\nabla\psi^{(0)} = \nabla\bar{\Phi}^{1/2} = 0$. The calculation of the complex integrals $\int_S\psi^{(1)}\,dS$ and $\int_V\psi^{(1)}\,dV$ is reported in Appendix B. Combining eqs 10 with the asymptotic formulas calculated in Appendix B, one finds $U_V^{(1)} = \int_V\psi^{(1)}\,dV = 0$, while the surface contribution $U_S^{(1)} = \int_S\psi^{(1)}\,dS$ to the energy of interaction between two disks set a distance $w_{jl}$ apart is

$$U_S^{(1)} \cong -\frac{3}{2}\pi a\frac{\gamma^2A^4}{k_BT}\bar{\Phi}\sum_{j=1}^{M}\sum_{l=1}^{M}e^{-\nu w_{jl}}/w_{jl} \qquad \nu A \to 0 \tag{11a}$$

$$\cong -\frac{1}{8\sqrt{3}}a^4\frac{\gamma^2A}{k_BT}\bar{\Phi}^{1/2}\varphi^{-3/2}\sum_{j=1}^{M}\sum_{l=1}^{M}e^{-\nu(w_{jl}-2A)}/w_{jl} \qquad \nu A \to \infty \tag{11b}$$

where $\nu \equiv (12\varphi\bar{\Phi}/a^2)^{1/2}$ and the relationship $\kappa^{(1)} = 6\gamma a/k_BT$ has been used. In a $\Theta$ solvent ($\nu \propto \varphi^{1/2} = 0$), $U_S^{(1)}$ simply reduces to $-(\gamma^2A^4a/k_BTw_{jl})$; namely, when a

semidilute polymer solution is in contact with a patched fluid membrane, two membrane patches, weakly interacting with the polymer, attract each other, the energy decaying as $w_{jl}^{-1}$. Moreover, the interaction strongly increases with disks' radius $A$ (rough as $A^4$), whereas it is reduced by excluded volume effects. For a uniform distribution of identical disks onto a plane, we may replace the double summation in eqs 11 by an integration over the whole surface. Assuming a uniform distribution function $\rho(w)$ around a generic disk

$$\rho(w) = \begin{array}{cc} 0 & w < 2A \\ \dfrac{1}{\pi(\bar{w}/2)^2} & w > 2A \end{array} \qquad (12)$$

$\bar{w}$ being the mean distance among the disks, integration of eqs 11 yields

$$\frac{1}{M}U_S^{(1)} \cong -6\pi a \frac{\gamma^2 A^4}{\nu k_B T \bar{w}^2}\bar{\Phi} e^{-2\nu A} \qquad \nu A \to 0 \qquad (13a)$$

$$\cong -\frac{1}{2\sqrt{3}} a^4 \frac{\gamma^2 A}{\nu k_B T \bar{w}^2}\bar{\Phi}^{-1/2}\varphi^{-3/2} \qquad \nu A \to \infty \qquad (13b)$$

Introducing the disk density $\rho = 1/\pi(\bar{w}/2)^2 = 1/S$, $S$ being the averaged surface area occupied by a single disk, the chemical potential $\mu$ can be written as a sum of a mixing entropy term[20] plus an interaction contribution:

$$\mu = -\alpha(T)\rho + k_B T \log \frac{\rho}{1 - B\rho} \qquad (14)$$

where $B \equiv \pi A^2$ is the excluded surface and $\alpha(T)$ is the polymer-induced energy of interaction defined as $(3/2)\pi^2$-$(a\gamma^2 A^4 \bar{\Phi}/\nu k_B T)e^{-2\nu A}$ when $\nu A \to 0$ and $(\pi/8\sqrt{3}(a^4\gamma^2 A/\nu k_B T \varphi^{3/2}\bar{\Phi}^{1/2})$ when $\nu A \to \infty$. Since the pressure $P$ is related to $\mu$ via[20] $(\partial P/\partial\rho)_T = \rho(\partial\mu/\partial\rho)_T$, we find $P = \int_0^\rho(-\alpha(T)\rho + k_B T(1 - B\rho)^{-1}\, d\rho = -(1/2)\alpha(T)\rho^2 - (k_B T/B)\log(1 - B\rho)$. For low disk density $B\rho \propto (A/\bar{w})^2 \ll 1$; hence $\log(1 - B\rho) \cong -B\rho/(1 - (1/2)B\rho) = -B/(S - (1/2)B)$, and therefore, after simple rearrangement

$$\left(P + \frac{\alpha(T)}{2S^2}\right)\left(S - \frac{1}{2}B\right) = k_B T \qquad (15)$$

which is nothing but the van der Waals equation of state for a two-dimensional gas of hard disks. The parameter $B$ is a purely geometrical term ($B \equiv \pi A^2$) while the parameter $\alpha(T)$ accounts for the polymer-mediated temperature-dependent attractive force between the disks. No direct interactions among the disks have been considered so far. If repulsive forces due, for instance, to the electrostatic charges of disk-forming lipids are inserted, the net effect is a numerical reduction of the $\alpha(T)$ parameter. Equation 15 predicts a phase separation from a gaslike to a condensed state of densely packed disks. The onset of phase separation requires that $(\partial P/\partial S)_T = (\partial^2 P/\partial S^2)_T = 0$. Simple algebra yields the following results for the critical temperature $T_C$

$$k_B T_C \propto a\gamma A(\bar{\Phi}/\varphi)^{1/4} \qquad \nu A \to 0 \qquad (16a)$$

$$\propto a^{5/2}(\gamma/\varphi)(\bar{\Phi}A)^{-1/2} \qquad \nu A \to \infty \qquad (16b)$$

Summing up, the main predictions of our model are

(a) In a $\Theta$ solvent the energy of interaction between two disks (i.e., isolated molecule or clusters) set a distance $w$ apart is always attractive, slowly decaying as $1/w$ (eq 11a).

(b) By introducing excluded volume interactions $\varphi$ among the polyelectrolyte chains, the behavior becomes more complex, the attractive component now decays faster than in the ideal chain case (roughly as $e^{-\nu w}/w$, where $\nu \equiv (12\varphi\bar{\Phi}/a^2)^{1/2}$). It is generally accepted that the screened electrostatic potential of the polyelectrolytes strongly contributes to the quite large values of $\varphi$. Local interactions, say H-bonds, may counteract this effect.

(c) Polymer-induced attractive forces among membrane patches are likely weak. Extensive aggregation of patches leading to mesoscopic domains may occur when the attraction forces balance the entropic ones. According to our estimate, eq 16, the critical temperature for phase separation is higher for strong lipid patch−polymer interactions $\gamma$ as well as for weak excluded volume interactions $\varphi$ among polymer chains.

(d) In a polyelectrolyte solution, excluded volume interactions can be reduced by salt addition. However, at high ionic strength also the polymer−charged lipid interactions (described by the phenomenological parameter $\gamma$) are weakened. Since polymer-induced attractive force scales as $\gamma^2$ (eqs 11), we may suppose that salt produces opposite effects. Our preliminary calorimetric data (see the next section) seem to support such a conjecture.

(e) Polymer-mediated forces among clusters (disks) strongly depend on disk radius $A$. The force roughly scales as $A^4$ when $\nu A \to 0$ (small disks and/or small excluded volume interactions, eq 11a) and as $Ae^{2\nu A}$ in the limit $\nu A \gg$ (i.e., large disks and strong excluded volume interactions, eq 11b). The consequences on patching kinetics should be interesting. Indeed, according to the above picture, the aggregation process should exhibit a long latency period owing to the weak attraction among small patches. Once they have reached a certain critical size, their mutual attraction becomes stronger and stronger, eventually leading to a burst in the clustering kinetics.

(f) In the case of semidilute ideal chains the model predicts a linear increase of the attractive forces with polymer concentration $\bar{\Phi}$ (eq 11a). The inclusion of repulsive forces among the chains weakens this dependence, and in the limit of strong excluded volume interactions, the force among the clusters may even decrease on further raising the polymer volume fraction (eq 11b).

## 4. Calorimetric Results

Preliminary calorimetric measurements lend strong support to the above theoretical findings. The rationale of our experiments is as follows. Lipid bilayers undergo a phase transition due to the cooperative melting of their hydrocarbon chains.[21] The phase transition temperature and its associated enthalpy can be easily detected even by low-sensitivity differential scanning calorimetry (DSC) through the plot of the specific heat vs temperature. The thermotropic behavior strongly depends on the lipid structure. In a random mixture of two different lipids the specific heat jump associated with the chain melting is broad, taking a typical shape as calculated by different authors.[21] On an increase in the incompatibility between the two components, the system approaches a mesoscopic lateral phase separation, forming transient, fluctuating microdomains richer in one component. Eventually, the system separates

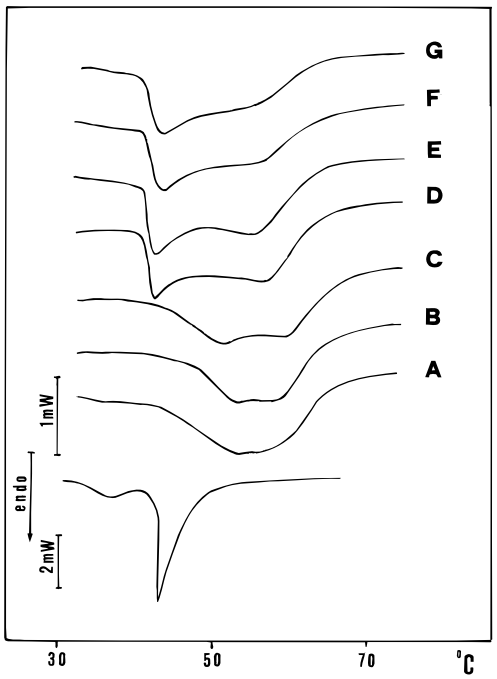


**Figure 3.** Specific heat (arbitrary units) vs temperature (°C) for DPPC/DPPA mixed bilayers (mole ratio 80:20) interacting with an aqueous solution of poly(L-lysine). The thermograms report the effect of increasing polyelectrolyte concentration $\bar{\Phi}$ (volume fraction): (A) $\bar{\Phi} = 0$; (B) $\bar{\Phi} = 0.002$; (C) $\bar{\Phi} = 0.004$; (D) $\bar{\Phi} = 0.02$; (E) $\bar{\Phi} = 0.04$; (F) $\bar{\Phi} = 0.08$; (G) $\bar{\Phi} = 0.16$. The first curve on the bottom is the specific heat of pure DPPC used as an internal standard for the temperature scale and transition enthalpy. No specific heat change was observed for pure poly(L-lysine) solutions in the range of investigated concentrations.

into two mesoscopic stable phases with different compositions. Small domains lead to a broadening of the calorimetric peak, whereas large clusters (of order of about $10^2-10^3$ lipid molecules) determine more complex patterns, eventually leading to the formation of a two-peak structure in the limit of mesoscopically large "phases" (length scale $\geq 10^{-2}-10^{-1}$ $\mu$m). Hences, the splitting of the calorimetric peak can be used as a tool to reveal the formation of large patches in multicomponent lipid bilayers.

The main DSC results are reported in Figure 3. At low polyelectrolyte concentrations the calorimetric peak of the DPPC/DPPA mixed bilayer is broader than those associated with the pure components but does not evidence the formation of two separated phases with different lipid compositions. When the polymer concentration is raised, a net splitting of the specific heat profile is observed, which suggests the formation of two phases, one richer in DPPC (melting at a lower temperature), the other one richer in DPPA. Further raising of the polymer concentration to the semidilute regime does not appreciably change the morphology of the thermograms.

The effect of the ionic strength on the polyelectrolyte-induced lateral phase separation of bilayer lipid components is reported in Figure 4. As discussed above, salt causes two opposite effects: (a) the screening of charged lipid−polyelectrolyte interactions with a consequent reduced polymer ability to trigger lipid lateral phase separation; (b) the screening of the electrostatic interactions among polymer chains. This allows for higher polymer concentrations over the charged lipid surface (see Figure 1) which favors the lipid lateral phase separation. The compensation between these

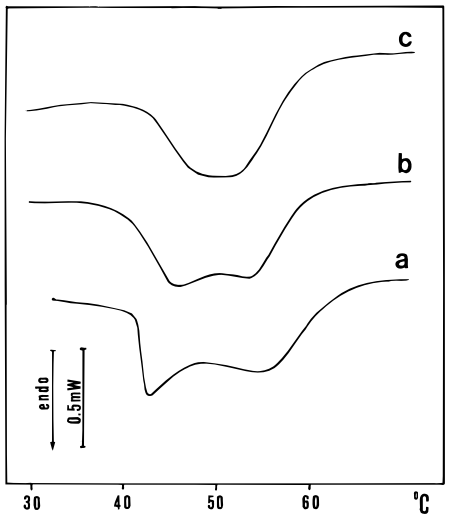


**Figure 4.** Effect of ionic strength on polymer-induced lateral phase separation in DPPC:DPPA (80:20) bilayers interacting with poly(L-lysine) ($\bar{\Phi} = 0.05$). The ionic strength was changed by NaCl: (a) no salt added; (b) NaCl = 0.05 M; (c) NaCl = 1 M.

opposite effects is evident in Figure 4, where the salt effect seems to be small, leading to a slight destabilization of the lipid clusters.

## 5. Concluding Remarks

The model we have developed suggests the existence of indirect polymer-mediated forces among clusters of like amphiphiles which are forming a fluid multicomponent interface with a polymer solution. The strength of these indirect interactions depends on several parameters such as size and distance of lipid clusters, polymer−lipid head group forces, polymer excluded volume, and temperature.

Scanning calorimetry has proven to be an effective tool in detecting patching thermodynamics and kinetics. However, a more detailed comparison between experiments and theory could be obtained through different techniques such as, for instance, fluorescence microscopy in Langmuir−Blodgett monolayers at the polymer solution−air interface or fluorescence quenching spectroscopy. These techniques have been able to detect even the finest geometrical details of heterogeneous multicomponent lipid assemblies ranging from the micrometer (fluorescence microscopy[22]) to the nanometer (fluorescence quenching spectroscopy[23]) range. Such methods could be very useful for measuring the onset of polymer-mediated forces in the crossover between dilute to semidilute polyelectrolyte solutions.

**Acknowledgment.** This work was partially supported by the Italian CNR and MURST. We would like to thank Prof. N. A. Mancini (CUMEC) for his kind permission to use the Mettler TA 3000 system.

## Appendix A

The aim of this appendix is to solve the integral equation (8)

$$\sum_{n=-\infty}^{+\infty} \int_0^{\infty} A_n^{(1)}(\lambda) J_n(\lambda r)(\lambda^2 + \nu^2)^{1/2} e^{+in\alpha}\, d\lambda = \begin{cases} \kappa^{(1)}\bar{\Phi}^{1/2} & r, \alpha \in I_A \\ 0 & r, \alpha \in I_B \end{cases} \quad \text{(A.1)}$$

where the domain $I_A$ defines the set of $r$ and $\alpha$ coordinates lying inside the circular disks of radius $A$ (see Figure 2) while the domain $I_B$ contains the remaining part of the surface. We multiply both sides of eq A.1 by $e^{-im\alpha}x^{1/2}J_m(xr)$, with $x$ a dummy variable $\infty > x > 0$, and integrate over $dS = r\,dr\,d\alpha$. Making use of the Hankel inverse theorem[24]

$$\int_0^\infty f(\lambda)(\lambda r)^{1/2}J_m(\lambda r)\,d\lambda\int_0^\infty (xr)^{1/2}J_m(xr)\,dr = \frac{1}{2}(f(x+0)+f(x-0)) \quad (A.2)$$

$f(x)$ being any arbitrary well-behaved function, eventually we find

$$A_m^{(1)}(x) = \frac{\kappa^{(1)}}{2\pi}\bar{\Phi}^{1/2}\frac{x}{(x^2+\nu^2)^{1/2}}\int_{r\in I_A} r\,dr\int_{\alpha\in I_A} J_m(xr)e^{-im\alpha}\,d\alpha \quad (A.3)$$

In the second step we express the variables $r$ and $\alpha$ within the adsorbing domains $I_A$ by means of a set of local variables, each of them has the origin at the center of a circular domain of radius $A$ which favorably interacts with the polymer (see Figure 2). Letting $\rho_j$ and $\beta_j$ be the new variables (where $j = 1, 2, ..., M$ denotes the generic $j$th disk), we may relate the old variables $r$ and $\alpha$ with the new ones $\rho_j$ and $\beta_j$ through simple trigonometric relationships:

$$r^2 = \rho_j^2 + r_{0j}^2 - 2\rho_j r_{0j}\cos\beta_j \quad (A.4a)$$

$$\cos(\alpha-\alpha_{0j}) = \frac{r_{0j}-\rho_j\cos\beta_j}{r} \quad (A.4b)$$

with $0 \le \rho_j \le A$ and $0 \le \beta_j \le 2\pi$. All the symbols have been defined in Figure 2 where the plane $X-Y$ stands for the membrane−water interface ($z = 0$) and $r_{0j}$ and $\alpha_{0j}$ are the polar coordinates of the center of the generic $j$th disk.

By introducing the new variables $\rho_j$ and $\beta_j$ into eq A.3, we transform the double integrals into a sum of definite integrals:

$$\int_{r\in I_A} r\,dr\int_{\alpha\in I_A} J_m(xr)e^{-im\alpha}\,d\alpha = \sum_{j=1}^{M}\int_0^A \rho_j\,d\rho_j\int_0^{2\pi} rJ_m(xr)e^{-im\alpha}|H|\,d\beta_j \quad (A.5)$$

where the Jacobian $|H|$ is

$$|H| = \begin{vmatrix} \frac{\partial r}{\partial\rho_j} & \frac{\partial r}{\partial\beta_j} \\ \frac{\partial\alpha}{\partial\rho_j} & \frac{\partial\alpha}{\partial\beta_j}\end{vmatrix} = \rho_j/r \quad (A.6)$$

In the third step we express the integrand as a function of the new variables $\rho_j$ and $\beta_j$. This can be made by expanding the integrand through a Fourier−Bessel series:[25]

$$rJ_m(xr)e^{-im\alpha} = r\exp(-im\alpha_{0j})J_m(xr)\exp(-im(\alpha-\alpha_{0j})) = r\exp(-im\alpha_{0j})\sum_{k=-\infty}^{+\infty}J_k(x\rho_j)J_{m+k}(xr_{0j})\exp(ik\beta_j) \quad (A.7)$$

This procedure allows one to transform eq A.4 into a more amenable form where the double integral is factorized

$$\int_{r\in I_A} r\,dr\int_{\alpha\in I_A} J_m(xr)e^{-im\alpha}\,d\alpha = \sum_{j=1}^{M}\sum_{k=-\infty}^{+\infty}\int_0^A\int_0^{2\pi}\exp(-im\alpha_{0j})J_k(x\rho_j)J_{m+k}(xr_{0j})\times \exp(ik\beta_j)\rho_j\,d\rho_j\,d\beta_j \quad (A.8)$$

The integration over $d\beta_j$ is trivial, and all the terms with $k \neq 0$ vanish; integrating over $d\rho_j$ with the aid of the relationship[26]

$$\int_0^A J_0(x\rho_j)\rho_j\,d\rho_j = \frac{A}{x}J_1(xA) \quad (A.9)$$

yields

$$\int_{r\in I_A} r\,dr\int_{\alpha\in I_A} J_m(xr)e^{-im\alpha}\,d\alpha = \frac{2\pi A}{x}J_1(xA)\sum_{j=1}^{M}\exp(-im\alpha_{0j})J_m(xr_{0j}) \quad (A.10)$$

where the sum spans over $M$ identical disks, the polar coordinates of their centers being $r_{0j}$ and $\alpha_{0j}$. Combining eqs A.3 and A.9 and interchanging the dummy variables ($x$ and $\lambda$, $n$ and $m$), we find an exact expression for the coefficients $A_m^{(1)}(\lambda)$ describing the polymer profile at the interface (eq 7 of the main text).

## Appendix B

From the polymer mass conservation constaint $\int_V\psi^2\,dV$ = constant together with the perturbation expansion $\psi = \bar{\Phi}^{1/2} + \psi^{(1)}$, it follows that $2\bar{\Phi}^{1/2}\int_V\psi^{(1)}\,dV = 0$. The remaining integral $\int_S\psi^{(1)}\,dS$, contained in eq 10 can be calculated by following the same procedure employed to obtain eq 9 and reported in Appendix A. Performing the proper changes of coordinates (eqs A4a,b), after some algebra one obtains

$$\int_S\psi^{(1)}\,dS = 2\pi\kappa^{(1)}A^2\bar{\Phi}^{1/2}\sum_{l=1}^{M}\sum_{j=1}^{M}\sum_{m=-\infty}^{+\infty}\int_0^\infty\frac{J_1^2(\lambda A)}{\lambda(\lambda^2+\nu^2)^{1/2}}\times J_m(\lambda r_{0j})J_m(\lambda r_{0l})\exp(im(\alpha_{0l}-\alpha_{0j}))\,d\lambda \quad (B.1)$$

Equation B.1 can be greatly simplified by noticing that[25]

$$\sum_{m=-\infty}^{+\infty}J_m(\lambda r_{0j})J_m(\lambda r_{0l})\exp(i(\alpha_{0l}-\alpha_{0j})) = J_0(\lambda|w_{jl}|) \quad (B.2)$$

where $|w_{jl}| \equiv |\vec{r}_{0j} - \vec{r}_{0l}| = (r_{0j}^2 + r_{0l}^2 - 2r_{0j}r_{0l}\cos(\alpha_{0l}-\alpha_{0j}))^{1/2}$ is the distance between the centers of $j$th and $l$th disk. Combining eqs B.1 and B.2, eventually we get

$$\int_S\psi^{(1)}\,dS = \frac{1}{2}2\pi\kappa^{(1)}A^2\bar{\Phi}^{1/2}\sum_{l=1}^{M}\sum_{j=1}^{M}\int_0^\infty\frac{J_1^2(\lambda A)}{\lambda(\lambda^2+\nu^2)^{1/2}}\times J_0(\lambda|w_{jl}|)\,d\lambda \quad (B.3)$$

(the factor $^1/_2$ has been introduced in order to avoid counting twice the interactions among the $j$th and $l$th clusters). In the ideal chain limit ($\Theta$ solvent) we may put $\nu \propto \nu^{1/2} = 0$ and the integral (B.3) has an exact compact analytical expression reported in Appendix C. In the more general case $\nu \neq 0$ the integral can be

approximately calculated as shown in Appendix C; asymptotic expressions are reported in eqs C8a,b.

## Appendix C

The aim of this appendix is the calculation of a family of integrals, $\zeta_m$, appearing in the calculation of the polymer adsorption energy onto a patched surface (eq B3):

$$\zeta_m \equiv \int_0^\infty \frac{J_1^2(\lambda A)}{\lambda(\lambda^2+\nu^2)^{m/2}} J_0(\lambda w)\, d\lambda \qquad (C.1)$$

where we used the notation $w \equiv |w_{jl}|$. $J_n(x)$ are Bessel functions and $m$ is a numerical constant ($m = 1$ in the present case).

Since $w$ (the distance between two disks, as shown in Figure 2) can be very large, $J_0(\lambda w)$ becomes a rapidly oscillating function which makes difficult the estimate of the (C.1) integral, even at the numerical level. Therefore, it is useful to transform the above integral by the following relationships:[26]

$$\frac{1}{(\lambda^2+\nu^2)^{1/2}} = \int_0^\infty e^{-\nu\rho} J_0(\lambda\rho)\, d\rho \qquad (C.2a)$$

$$\frac{\pi}{4\lambda A} J_1^2(\lambda A) = \int_0^1 x(1-x^2)^{1/2} J_1(2\lambda A x)\, dx \qquad (C.2b)$$

Inserting eqs C.2a,b into eq C.1 and rearranging yield

$$\zeta_1 = \int_0^\infty d\lambda \int_0^\infty d\rho \int_0^1 [x(1-x^2)^{1/2} e^{-\nu\rho} J_0(\lambda\rho) J_0(\lambda w) J_1(2\lambda A x)]\, dx \qquad (C.3)$$

The integration over $d\lambda$ can be carried out analytically:[26]

$$\int_0^\infty J_0(\lambda\rho) J_0(\lambda w) J_1(2\lambda A x)\, d\lambda = \frac{1}{2\pi A x} \arccos\left(\frac{w^2+\rho^2-4A^2x^2}{2w\rho}\right) \quad w-2Ax < \rho < w+2Ax$$

$$= 0 \quad w+2Ax < \rho < \infty \text{ and } w-2Ax > \rho > 0 \qquad (C.4)$$

By exploiting the result reported in eq C.4, introducing the new variable $\epsilon$ defined as $\rho = (1+\epsilon)w$, and setting $\Delta \equiv 2A/w$, we get

$$\zeta_1 = \frac{2w}{\pi^2} e^{-\nu w} \int_{-\Delta x}^{+\Delta x} d\epsilon \int_0^1 (1-x^2)^{1/2} e^{-\nu w\epsilon} \arccos\left(\frac{1+(1+\epsilon)^2-\Delta^2x^2}{2(1+\epsilon)}\right) dx \qquad (C.5)$$

The integrand now is a smooth, well-behaved function which does not exhibit the disturbing rapid oscillations of the untransformed integral; moreover, for large $w$ both the variables $\epsilon$ and $\Delta$ are small quantities ($\Delta \equiv 2A/w$ and $-\Delta x \le \epsilon \le +\Delta x$, with $x \le 1$ and $w \ge 2A$), and this fact allows for a power series expansion:

$$\arccos\left(\frac{1+(1+\epsilon)^2-\Delta^2x^2}{2(1+\epsilon)}\right) \cong (\Delta^2x^2-\epsilon^2)^{1/2} + O(\Delta^3,\epsilon^3) \qquad (C.6)$$

Inserting eq C.6 into (C.5) and integrating twice over $d\epsilon$ and $dx$ (all the integrals have an exact analytical expression[26]), eventually we obtain

$$\zeta_1 \cong \frac{2w}{\pi^2} e^{-\nu w} \int_0^1 (1-x)^2 \int_{-\Delta x}^{+\Delta x} e^{-\nu w\epsilon} (\Delta^2x^2-\epsilon^2)^{1/2}\, d\epsilon\, dx = \frac{4}{\pi}\frac{A}{\nu w} e^{-\nu w} \int_0^1 x(1-x^2)^{1/2} I_1(2\nu A x)\, dx = \frac{1}{4}\frac{1}{\nu^2 w} I_1^2(\nu A) e^{-\nu w} \qquad (C.7)$$

$I_1(z)$ being a modified Bessel function. Using the asymptotic expressions of $I_1(z)$ for small and large $z$ ($I_1(z) \cong z/2(1 + z^2/8 + ...)$ for $z \to 0$ and $I_1(z) \cong e^{+z}/(2\pi z)^{1/2}$ for $z \to \infty$), we may rewrite eq C.7 as

$$\zeta_1 \cong \frac{1}{16}\frac{A^2}{w} e^{-\nu w} \qquad \nu A \to 0 \qquad (C.8a)$$

$$\cong \frac{1}{8\pi}\frac{e^{-\nu(w-2A)}}{\nu^3 w A} \qquad \nu A \to \infty \qquad (C.8b)$$

It is worth noting that in the limit $\nu \to 0$ the result of eq C.8a can be compared with the exact analytical results obtained by setting in eq C.1 $\nu = 0$

$$\lim_{\nu\to 0}\zeta_1 = \int_0^\infty \frac{J_1^2(\lambda A)}{\lambda^2} J_0(\lambda w)\, d\lambda = \frac{A^2}{4w} F_4\left(\frac{1}{2},\frac{1}{2};2,2;\frac{A^2}{w^2},\frac{A^2}{w^2}\right) \qquad (C.9)$$

$F_4(\alpha,\beta;\gamma,\gamma';x,y)$ being a hypergeometric function of two variables[26] which is meaningful only if $w \ge 2A$ (non-overlapping disks). The hypergeometric function can be expressed through a double-series expansion:[26]

$$F_4(\alpha,\beta;\gamma,\gamma';x,y) = \sum_{m=0}^\infty \sum_{n=0}^\infty \frac{(\alpha)_{m+n}(\beta)_{m+n}}{(\gamma)_m(\gamma')_n m!n!} x^m y^n \qquad (C.10)$$

where Pochammer's symbols $(p)_m$ are defined by means of the Euler $\Gamma$ function as $(p)_m = \Gamma(p+m)/\Gamma(p)$. Combining eqs C.9 and C.10 yields

$$\lim_{\nu\to 0}\zeta_1 = \frac{A^2}{4w}\left(1 + \frac{A^2}{4w^2} + \frac{15}{64}\frac{A^4}{w^4} + ...\right) \qquad (C.11)$$

Since $w \ge 2A$, the convergence of the series (C.11) is very fast and a few terms are enough for practical purposes. The small difference in the numerical prefactor between eqs C.8a and C.11 is probably due to the power series expansion used in eq C.6.

## References and Notes


(1) Pali, T.; Horwath, L. I. *Biochim. Biophys. Acta* **1989**, *984*, 128.
(2) Laroche, G.; Dufourc, E. J.; Pezolet, M.; Dufourcq, J. *Biochemistry* **1990**, *29*, 6460.
(3) Maggio, B.; Sturtevant, J. M.; Yu, R. K. *J. Biol. Chem.* **1987**, *262*, 2652.
(4) Ikeda, T.; Yamaguchi, H.; Tazuke, S. *Biochim. Biophys. Acta* **1990**, *1026*, 105.
(5) Raudino, A.; Castelli, F.; Gurrieri, S. *J. Phys. Chem.* **1990**, *94*, 1526.
(6) Raudino, A.; Castelli, F. *Colloid Polym. Sci.* **1992**, *270*, 1116.
(7) Maksymiw, R.; Sui, S. F.; Gaub, H.; Sackmann, E. *Biochemistry* **1987**, *26*, 2983.
(8) Hartmann, W.; Galla, H. J.; Sackmann, E. *FEBS Lett.* **1977**, *78*, 169.
(9) Gaylord, R. J.; Zhang, H. *J. Chem. Phys.* **1987**, *86*, 440.
(10) Marcelja, S.; Radic, N. *Chem. Phys. Lett.* **1976**, *42*, 129.

(11) For a recent review see, e.g.: Mouritsen, O. G.; Sperotto, M. M. In *Thermodynamics of Membrane Receptors and Channels*; Jackson, M. B., Ed.; CRC Press: Boca Raton, FL, 1992; pp 127−181.
(12) See, e.g.: Leikin, S.; Parsegian, V. A.; Rau, D. C.; Rand, R. P. *Annu. Rev. Phys. Chem.* **1993**, *44*, 369.
(13) For a detailed account of the structure of DPPC and DPPA phospholipids see, e.g.: Cevc, G.; Marsh, D. *Phospholipid Bilayers*; Wiley: New York, 1987.
(14) Bartlett, G. R. *J. Biol. Chem.* **1959**, *234*, 466.
(15) de Gennes, P.-G. *Scaling Concepts in Polymer Physics*; Cornell University Press: Ithaca, NY, 1979.
(16) de Gennes, P.-G. *J. Chem. Phys.* **1980**, *72*, 4756.
(17) Roe, R. J. *Macromolecules* **1986**, *19*, 728.
(18) Tang, H.; Freed, K. F. *J. Chem. Phys.* **1991**, *94*, 6307.
(19) Szleifer, I.; Widom, B. *J. Chem. Phys.* **1989**, *90*, 7524.
(20) Israelachvili, J. N. *Intermolecular and Surface Forces*; Academic Press: London, 1985.
(21) For a review of early works see, e.g., ref 13; among recent papers we quote: Risbo, J.; Sperotto, M. M.; Mouritsen, O. G. *J. Chem. Phys.* **1995**, *103*, 3643.
(22) McConnell, H. M. *Annu. Rev. Phys. Chem.* **1991**, *42*, 171.
(23) See, e.g.: Silvius, J. R. *Biochemistry* **1992**, *31*, 3398 and references therein.
(24) Sneddon, I. N. *Mixed Boundary Value in Potential Theory*; North-Holland: Amsterdam, 1966.
(25) Abramowitz, M.; Stegun, I. *Handbook of Mathematical Functions*; Dover: New York, 1972.
(26) Gradshteyn, I. S.; Ryzhik, I. M. *Tables of Integrals, Series and Products*; Academic Press: New York, 1980.

MA960904Y